Electronic Supplementary Material (ESI) for Materials Chemistry Frontiers.
This journal is © the Partner Organisations 2021

Supporting Information

Transparent Photodetector Based on Polyoxometalate Modified Electrospun ZnO Homojunction Nanowires Intersection Array

Yuxiao Zheng,[a] Xueying Xu,[a] Fengrui Li,[a] Weilin Chen,*[a] Jian Gong,*[a] Chunlei Wang,[b]

[a] Key Laboratory of Polyoxometalate and Reticular Material Chemistry of Ministry of Education, Faculty of Chemistry, Northeast Normal University, Changchun, 130024, China, E-mail addresses: chenwl@nenu.edu.cn

[b] Library of Northeast Normal University, Changchun, 130024, China

Experimental method:

Synthesis of $Na_8[HPW_9O_{34}]$ (PW_9)[1]: Add 120 g of $NaWO_4{\cdot}2H_2O$ to 150 mL of deionized water, stir vigorously to dissolve it completely, and then add 3 mL of H_3PO_4 and 22 mL of glacial acetic acid in sequence. After vigorous stirring, the solution becomes turbid, and it becomes white after suction filtration. The crystal precipitation $Na_8[HPW_9O_{34}]$, the structure diagram of its polyacid anion is shown in Figure S1.

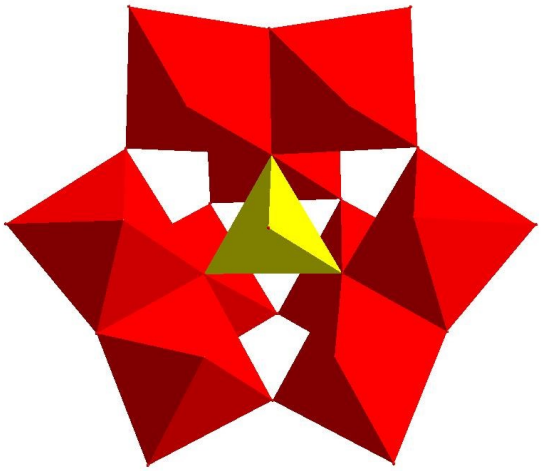

Figure S1. PW_9 anion structure diagram.

Synthesis of $Na_7[PW_{11}O_{39}]$ (PW_{11})[2]: Add 72.5 g of $NaWO_4{\cdot}2H_2O$ and 2.84 g of $Na_2HPO_4{\cdot}2H_2O$ to 200 mL of deionized water, heat the solution to 80 ~ 90°C, and adjust the pH to 4.8 with concentrated nitric acid under vigorous stirring, then continue to heat and evaporate about 100 mL of the solvent, then cool to room temperature and extract with 100 mL of acetone. Repeat the extraction until the solution no longer contains nitrate ions, and finally a white precipitate $Na_7[PW_{11}O_{39}]$ is obtained. The acid anion structure is shown in Figure S2.

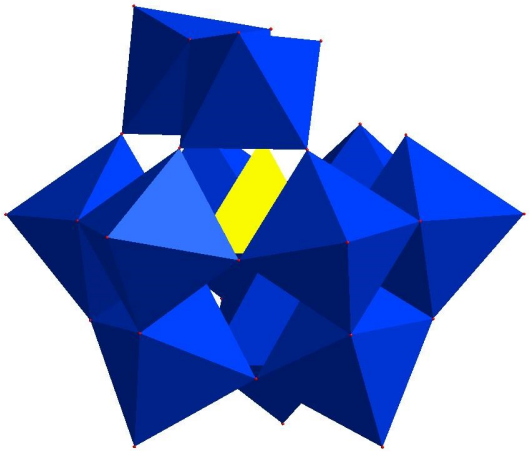

Figure S2. PW_{11} anion structure diagram.

Synthesis of $H_3[PW_{12}O_{40}]$ $(PW_{12})^3$: Add 25 g of $NaWO_4 \cdot 2H_2O$ and 4 g of $Na_2HPO_4 \cdot 2H_2O$ to 150 mL of deionized water at 80 ~ 90°C. The solution is slightly turbid. Under vigorous stirring, add 25 mL of concentrated hydrochloric acid dropwise to the solution. At this time, the solution becomes clear. If the solution is light blue, add 1 to 2 drops of 3% hydrogen peroxide to the solution to make the solution clear. Continue heating for 30 s and then cool to room temperature. Transfer the solution in the beaker and a small amount of precipitated solids to a separatory funnel. Add 35 mL of ether to the separatory funnel for extraction, and then add 10 mL of 6 mol / L HCl for shaking. Remove the oily substance from the lower layer and heat it to evaporate in a water bath to obtain light yellow crystals $H_3[PW_{12}O_{40}]$. The structure of the polyacid anion is shown in Figure S3.

Figure S3. PW_{12} anion structure diagram.

Figure S4. Photograph of PW11@ZnO NWs photodetector.

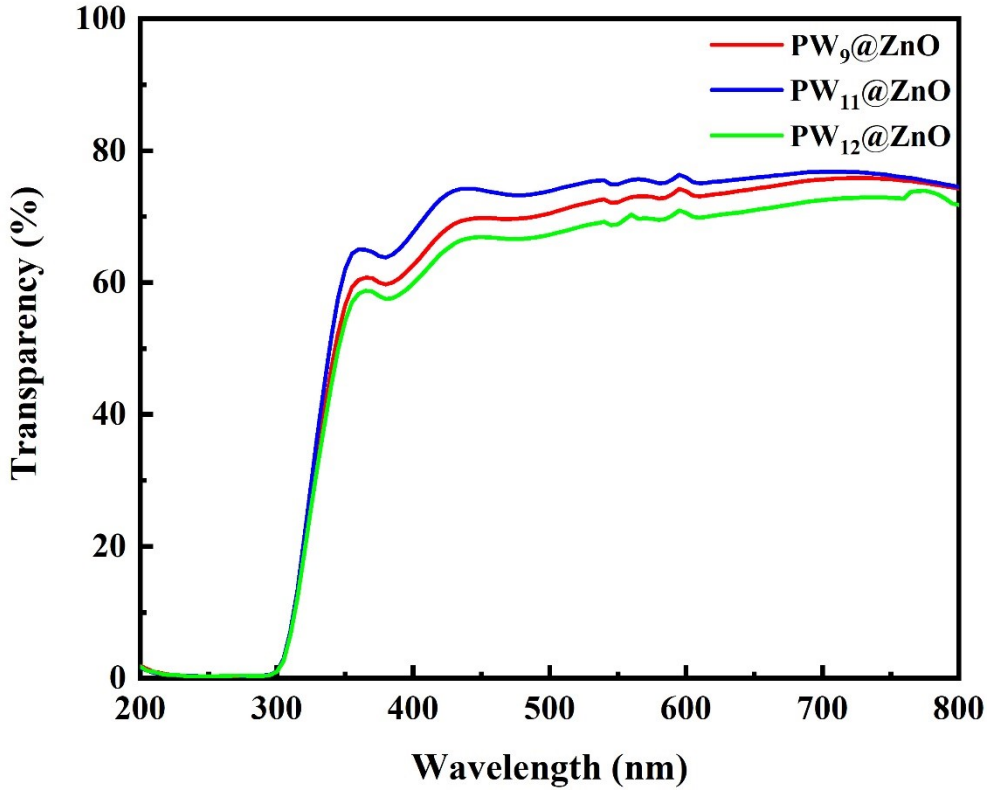

Figure S5. Light transmittance of POMs@ZnO NWs device.

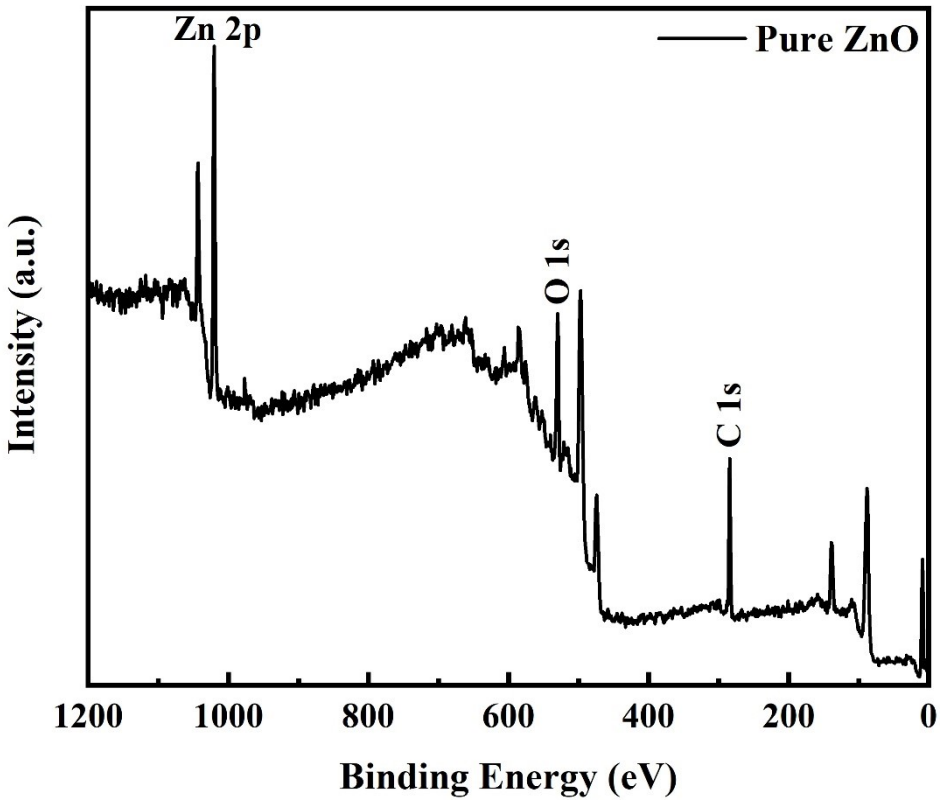

Figure S6. XPS full spectrum of pure ZnO NWs.

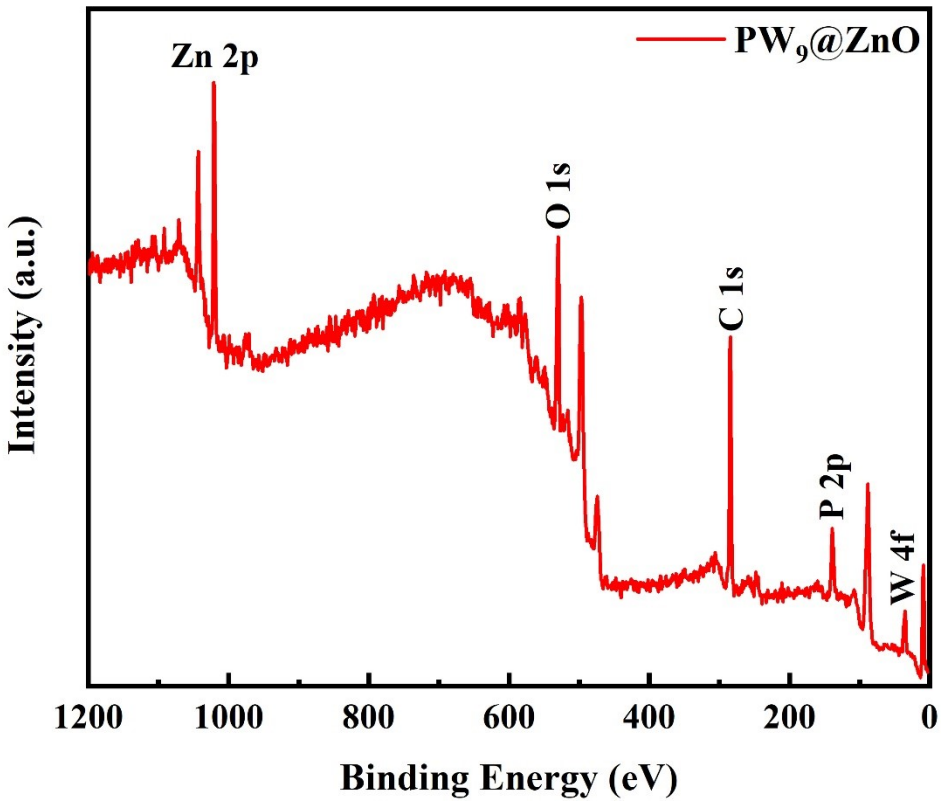

Figure S7. XPS full spectrum of PW_9@ZnO NWs.

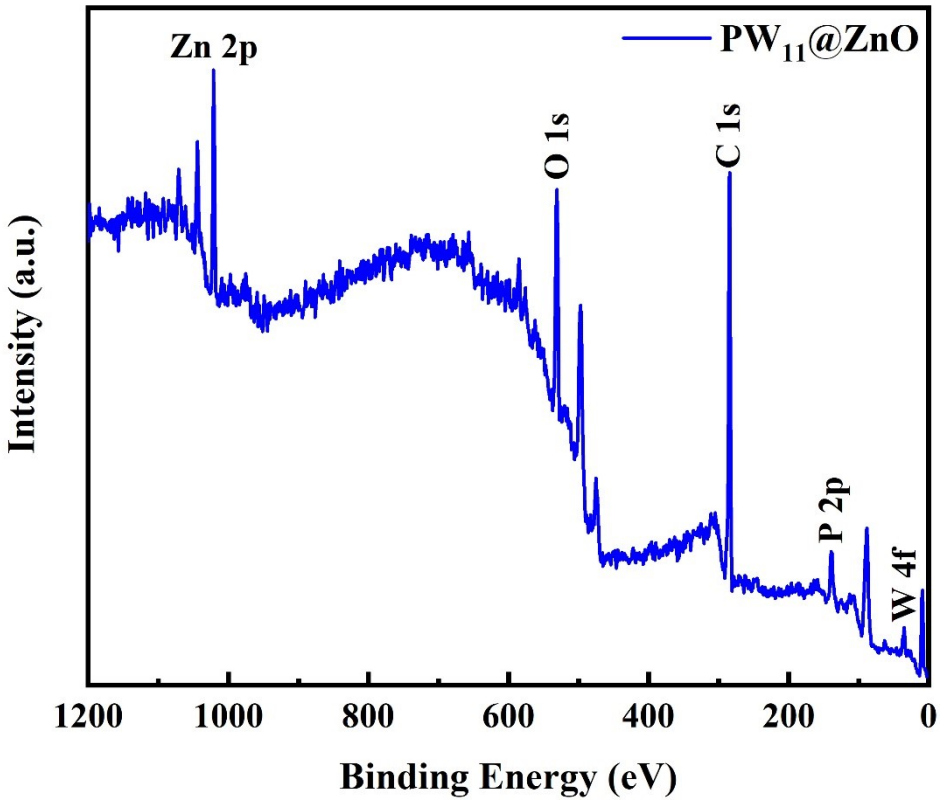

Figure S8. XPS full spectrum of PW_{11}@ZnO NWs.

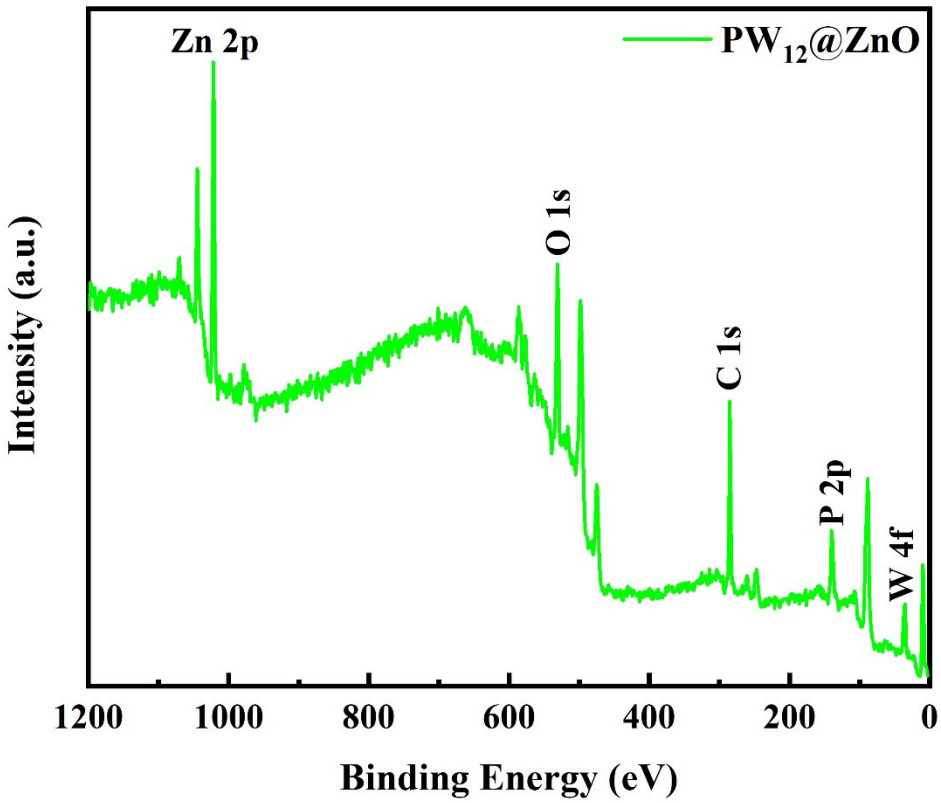

Figure S9. XPS full spectrum of PW_{12}@ZnO NWs.

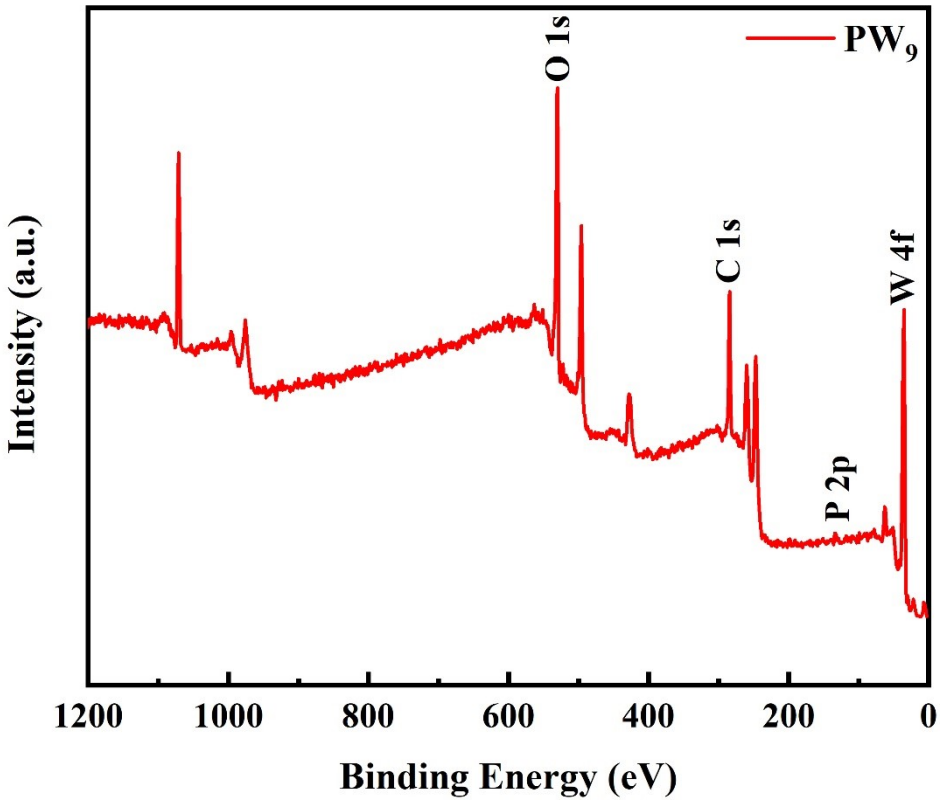

Figure S10. XPS full spectrum of pure PW_9.

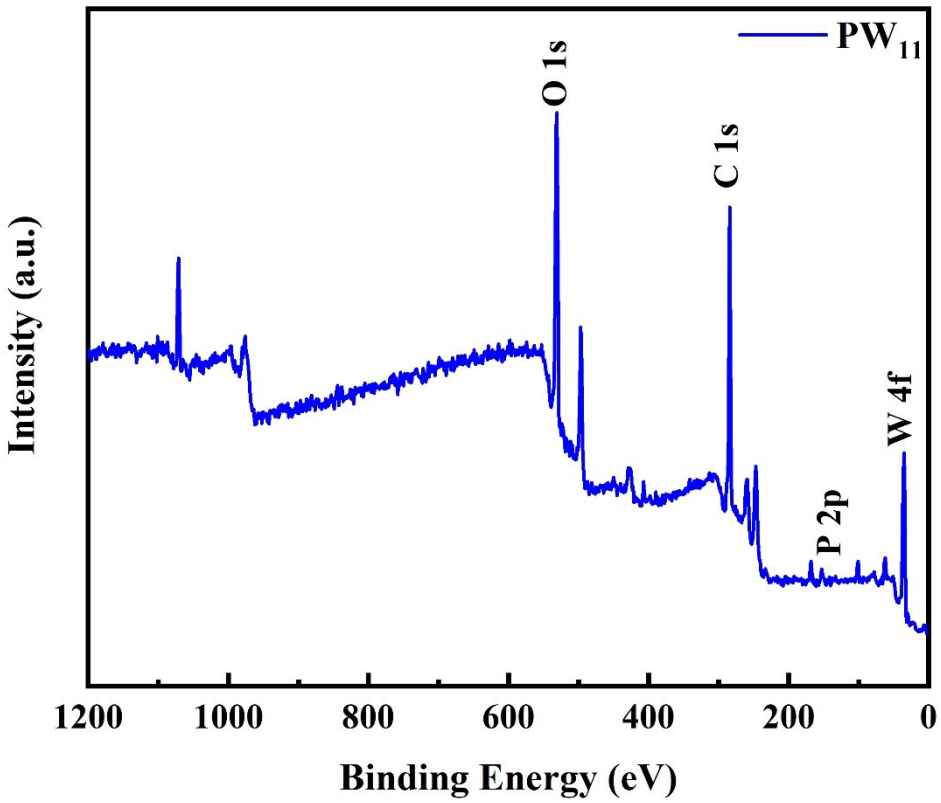

Figure S11. XPS full spectrum of pure PW_{11}.

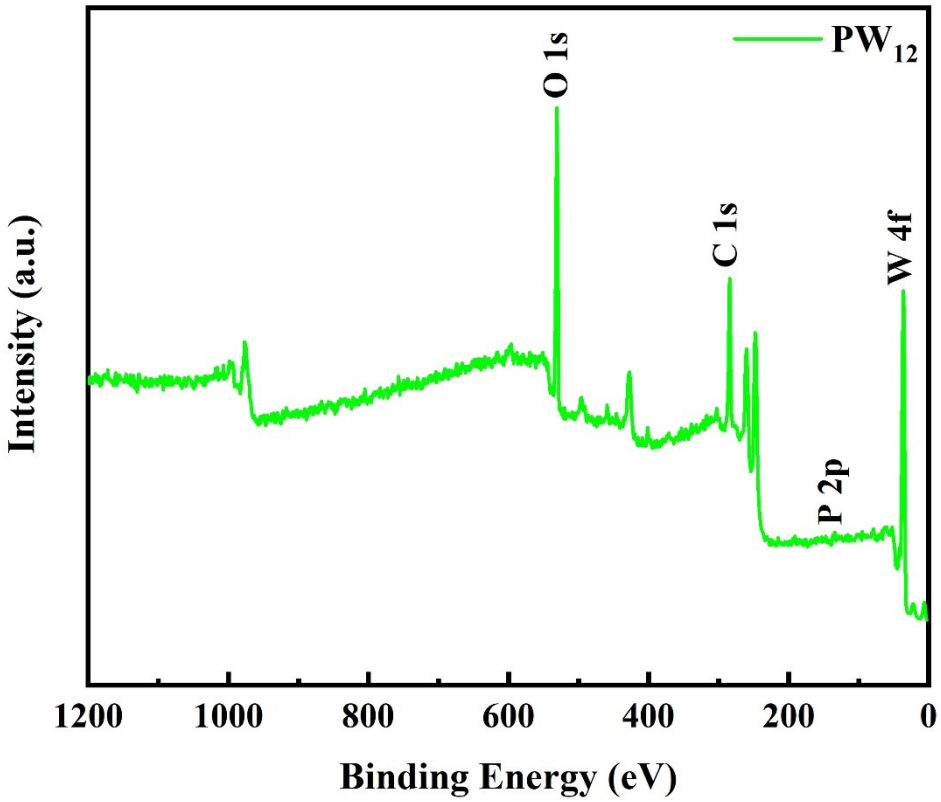

Figure S12. XPS full spectrum of pure PW_{12}.

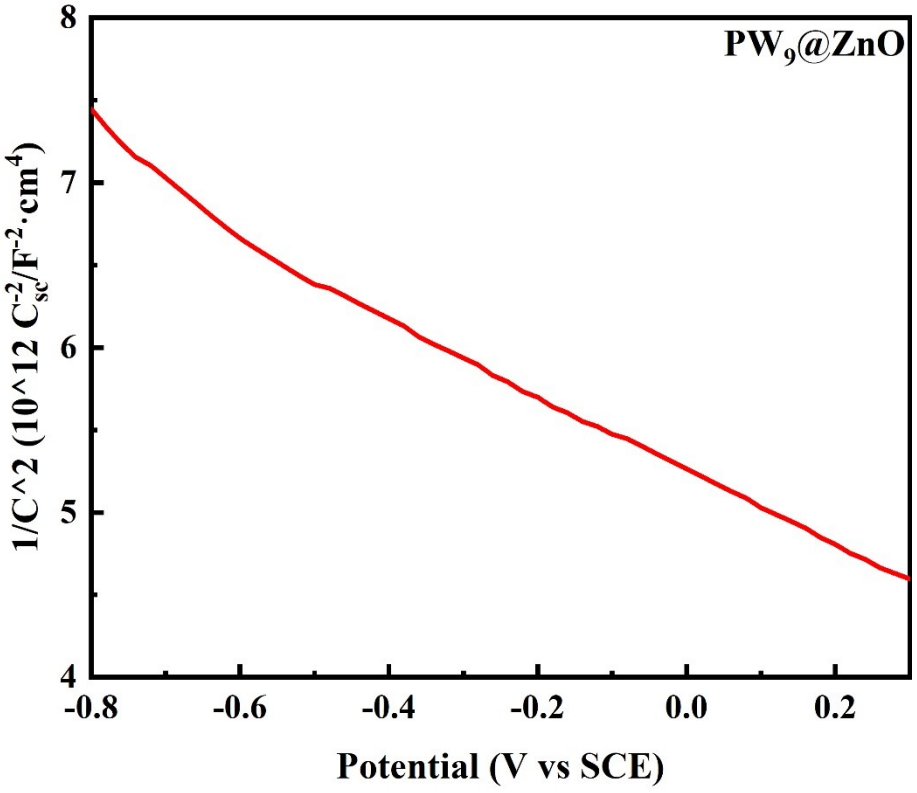

Figure S13. Mott-Schottky curve of PW_9@ZnO NWs.

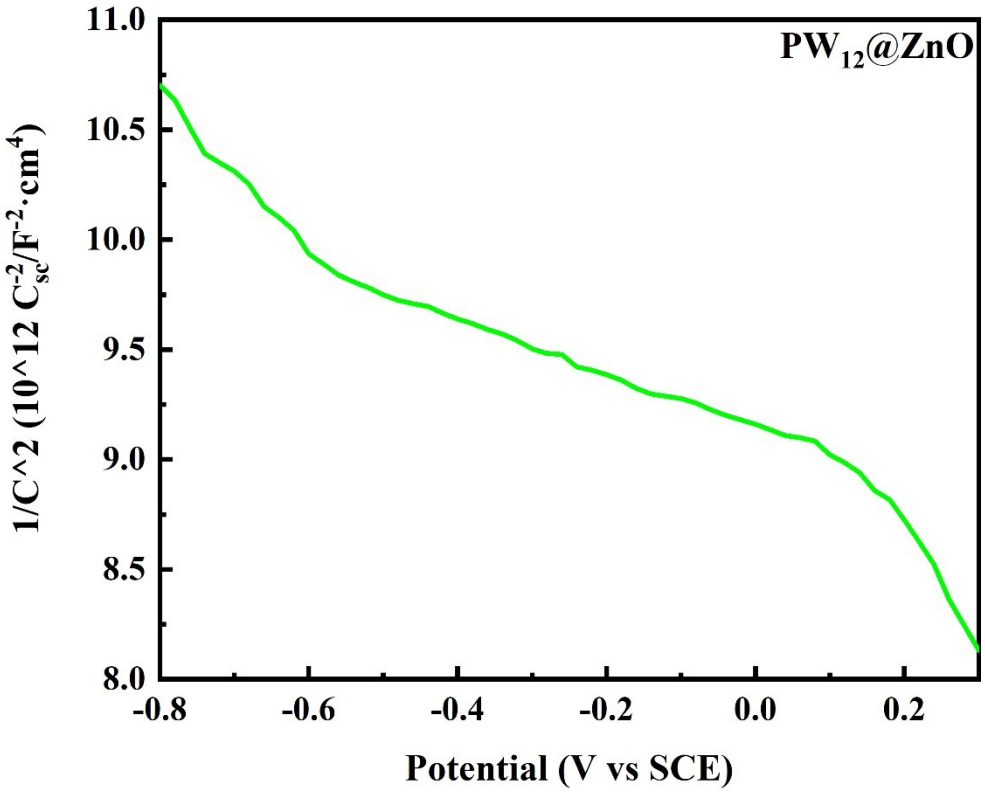

Figure S14. Mott-Schottky curve of PW_{12}@ZnO NWs.

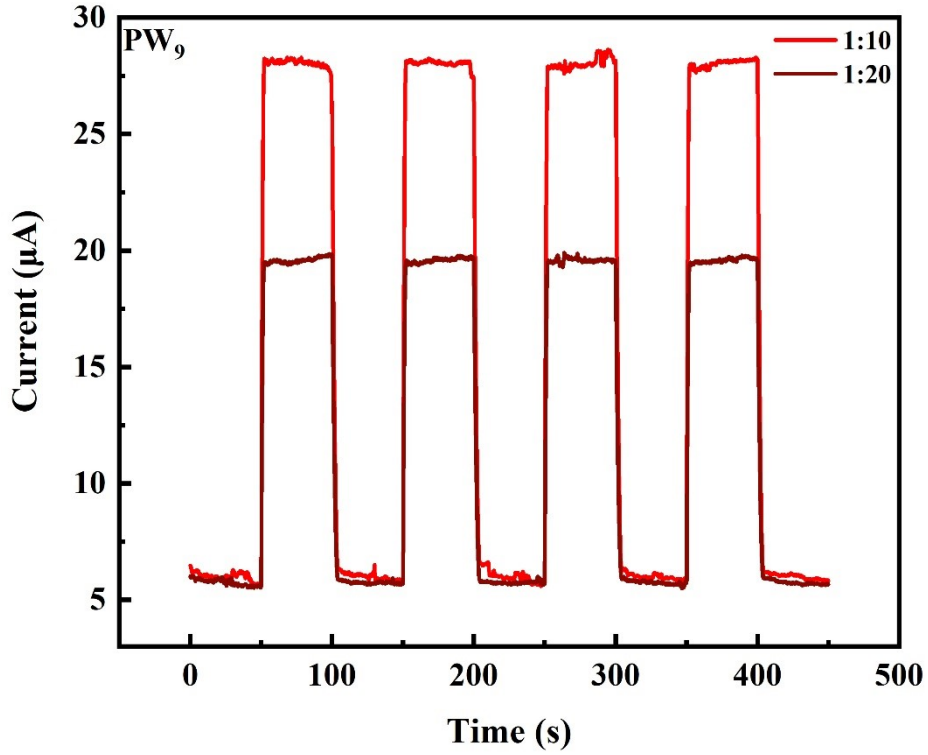

Figure S15. The I-t curve of the photodetector when the mass doping ratio of PW_9 is 1:10 and 1:20 (spinning time 1 min).

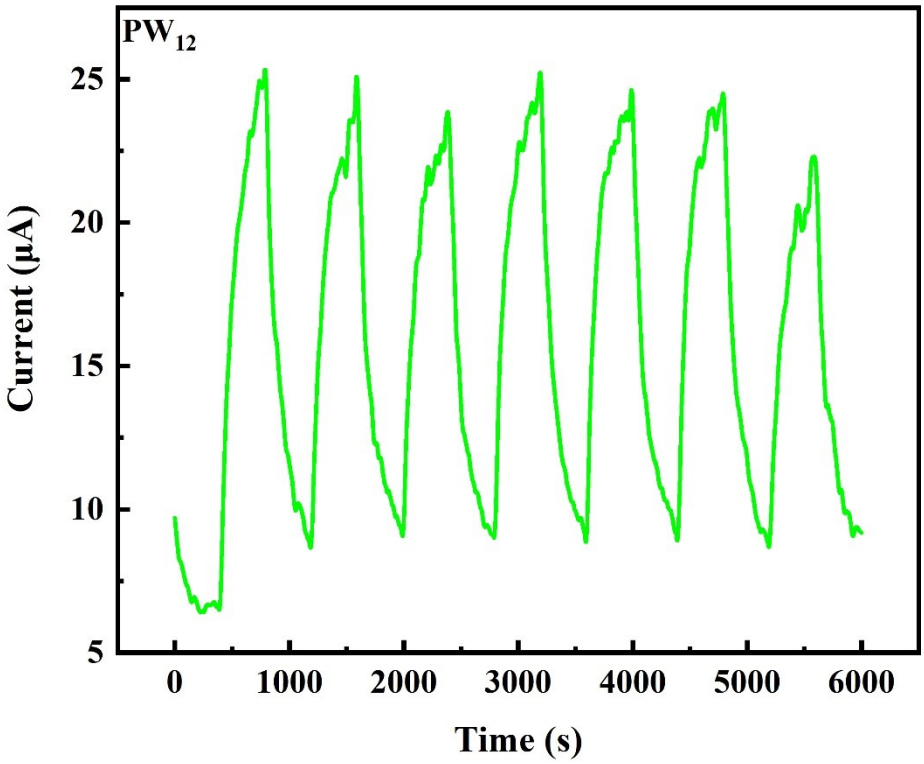

Figure S16. I-t curve of the photodetector when the mass doping ratio of PW_{12} is 1:15 (spinning time 1 min).

Table S1. Comparison of characteristic parameters of ZnO-based UV PDs.

Photodetector	Bias	Power density	Darkcurrent	Photocurrent	On–off ratio	ΔI	Rise time	Decay time	Transparency	Method	Ref.
ZnO nanofibers	1 V	77.5 μW·cm^{-2}	20 pA	6.5 μA	3.3 × 10^{5}	6.5 μA	≈100 s	≈50 s	-	Electrospinning	4
ZnO homojunction (Li-doped)	-10 V	25 mW·cm^{-2}	3.6 μA	19.5 μA	5.4	15.9 μA	-	-	-	Hydrothermal	5
ZnO homojunction (Cu-doped)	-5 V	0.25 mW·cm^{-2}	112 nA	602 nA	5.4	490 nA	≈50 s	≈200 s	-	CVD	6
ZnO homojunction (Sb-doped)	-3 V	60 mW·cm^{-2}	28.3 μA	930 μA	33	901.7 μA	15.2 s	20.3 s	-	Hydrothermal	7
Ag-doped ZnO nanowire	-	15-20mW·cm^{-2}	0.1 nA	5.2 nA	52	5.1 nA	1.09 s	5 s	-	Electrochemical deposition	8
ZnO thin film–Cu nanowires	0 V 1 V	0.8 mW·cm^{-2}	1 pA 30 pA	70 pA 2.95 nA	70 98	69 pA 2.95 nA	1 s 10.35 s	30 s 2 s	-	Spincoating	9
ZnO-SnO_2 NWs	10 V	0.45 mW·cm^{-2}	1.7 pA	7.9 nA	4.6 × 10^{3}	7.9 nA	32.2 s	7.8 s	>70%	Electrospinning	10
ZnO ultraporous film	5 V	100 μW·cm^{-2}	3.6 nA	1.2 mA	3.3 × 10^{5}	1.2 mA	250 s	150 s	-	Fame spray pyrolysis	11
ZnO homojunction nanofibers	0 V	2.5 mW·cm^{-2}	0.02 pA	0.5 nA	2.5 × 10^{4}	0.5 nA	3.9 s	4.7 s	89%	Electrospinning	12
Cu-Cu2O / ZnO(heating)	0 V	70 mW·cm^{-2}					3.89 ms	4.12 ms	>80%	Magnetron sputtering	13
POMs@ZnO NWs	0 V	100 mW·cm^{-2}	5.05 μA	28.81 μA	5.7	23.76 μA	1.32 s	2.62 s	>70%	Electrospinning	This work

Table S2. The area under the deconvoluted subpeaks from the high-resolution O1s spectra of ZnO and PW_{11}@ZnO.

	O_1	O_2	O_{total}	$O_{lattice}(O_1/O_{total})$	$O_{O-H}(O_2/O_{total})$	$O_{O-H}/O_{lattice}$
ZnO	8800	10000	18800	0.468	0.532	1.136
PW_{11}@ZnO	4250	17000	21250	0.2	0.8	4

references

1. W.H. Fang, W.D. Wang, G.Y. Yang. A novel poly(polyoxometalate) built by $\{Cu_9\}/\{Cu_5\}$ clusters and $\{PW_9\}/\{PW_{10}\}/\{PW_{11}\}$ lacunary fragments. *Dalton T.*, 2015, **44**, 12546-12549.
2. H. Wang, L. Fang, Y. Yang, R. Hu, Y. Wang. Immobilization $Na_7PW_{11}O_{39}$ on quanternary ammonium functionalized chloromethylated polystyrene by electrostatic interactions: An efficient recyclable catalyst for alcohol oxidation. *Appl. Catal. A-Gen.*, 2016, **520**, 35-43.
3. H. Shi, T. Zhao, J. Wang, Y. Wang, Z. Chen, B. Liu, et al. Fabrication of g-C_3N_4/PW_{12}/TiO_2 composite with significantly enhanced photocatalytic performance under visible light. *J. Alloy. Compd.*, 2021, **860**, 157924.
4. X. Liu, L. Gu, Q. Zhang, J. Wu, Y. Long, Z. Fan. All-printable band-edge modulated ZnO nanowire photodetectors with ultra-high detectivity. *Nat. Commun.*, 2014, **5**, 4007.
5. W. Ko, S. Lee, N. Myoung, J. Hong. Solution processed vertically stacked ZnO sheet-like nanorod p–n homojunctions and their application as UV photodetectors. *J Mater. Chem. C*, 2016, **4**, 142-149.
6. C.L. Hsu, Y.D. Gao, Y.S. Chen, T.J. Hsueh. Vertical p-type Cu-doped ZnO/n-type ZnO homojunction nanowire-based ultraviolet photodetector by the furnace system with hotwire assistance. *ACS Appl. Mater. Inter.*, 2014, **6**, 4277-4285.
7. W. Dai, X. Pan, S. Chen, C. Chen, W. Chen, H. Zhang, et al. ZnO homojunction UV photodetector based on solution-grown Sb-doped p-type ZnO nanorods and pure n-type ZnO nanorods. *RSC Adv.*, 2015, **5**, 6311-6314.
8. O. Lupan, V. Cretu, V. Postica, M. Ahmadi, B.R. Cuenya, L. Chow, et al. Silver-doped zinc oxide single nanowire multifunctional nanosensor with a significant enhancement in response. *Sensor. Actuat. B-Chem.*, 2016, **223**, 893-903.
9. F. Teng, L. Zheng, K. Hu, H. Chen, Y. Li, Z. Zhang, et al. A surface oxide thin layer of copper nanowires enhanced the UV selective response of a ZnO film photodetector. *J Mater. Chem. C*, 2016, **4**, 8416-8421.
10. W. Tian, T. Zhai, C. Zhang, S.L. Li, X. Wang, F. Liu, et al. Low-cost fully transparent ultraviolet photodetectors based on electrospun ZnO-SnO2 heterojunction nanofibers. *Adv. Mater.*, 2013, **25**, 4625-4630.
11. N. Nasiri, R. Bo, F. Wang, L. Fu, A. Tricoli. Ultraporous Electron-Depleted ZnO Nanoparticle

Networks for Highly Sensitive Portable Visible-Blind UV Photodetectors. *Adv. Mater.*, 2015, **27**, 4336-4343.

12. Y. Ning, Z. Zhang, F. Teng, X. Fang. Novel Transparent and Self-Powered UV Photodetector Based on Crossed ZnO Nanofiber Array Homojunction. *Small*, 2018, **14**, 1703754.
13. A.K. Rana, J.T. Park, J. Kim, C.-P. Wong. See-through metal oxide frameworks for transparent photovoltaics and broadband photodetectors. *Nano Energy*, 2019, **64**.